


# Depletion of adipocyte sphingosine kinase 1 leads to cell hypertrophy, impaired lipolysis, and nonalcoholic fatty liver disease

Andrea K. Anderson<sup>1,2,†</sup>, Johana M. Lambert<sup>1,2,†</sup>, David J. Montefusco<sup>1</sup>, Bao Ngan Tran<sup>1</sup>, Patrick Roddy<sup>3</sup>, William L. Holland<sup>4</sup>, and L. Ashley Cowart<sup>1,5,\*</sup> 

<sup>1</sup>Department of Biochemistry and Molecular Biology, Virginia Commonwealth University, Richmond, VA, USA, <sup>2</sup>Departments of Biochemistry and Molecular Biology Medical University of South Carolina, Charleston, SC, USA, <sup>3</sup>Department of Regenerative Medicine, Medical University of South Carolina, Charleston, SC, USA, <sup>4</sup>Department of Nutrition and Integrative Physiology, University of Utah, Salt Lake City, UT, USA, <sup>5</sup>Hunter Holmes McGuire Veterans Affairs Medical Center, Richmond, VA, USA

**Abstract** Sphingolipids have become established participants in the pathogenesis of obesity and its associated maladies. Sphingosine kinase 1 (SPHK1), which generates S1P, has been shown to increase in liver and adipose of obese humans and mice and to regulate inflammation in hepatocytes and adipose tissue, insulin resistance, and systemic inflammation in mouse models of obesity. Previous studies by us and others have demonstrated that global sphingosine kinase 1 KO mice are protected from diet-induced obesity, insulin resistance, systemic inflammation, and NAFLD, suggesting that SPHK1 may mediate pathological outcomes of obesity. As adipose tissue dysfunction has gained recognition as a central instigator of obesity-induced metabolic disease, we hypothesized that SPHK1 intrinsic to adipocytes may contribute to HFD-induced metabolic pathology. To test this, we depleted *Sphk1* from adipocytes in mice (SK1<sup>fatKO</sup>) and placed them on a HFD. In contrast to our initial hypothesis, SK1<sup>fatKO</sup> mice displayed greater weight gain on HFD and exacerbated impairment in glucose clearance. Pro-inflammatory cytokines and neutrophil content of adipose tissue were similar, as were levels of circulating leptin and adiponectin. However, SPHK1-null adipocytes were hypertrophied and had lower basal lipolytic activity. Interestingly, hepatocyte triacylglycerol accumulation and expression of pro-inflammatory cytokines and collagen 1a1 were exacerbated in SK1<sup>fatKO</sup> mice on a HFD, implicating a specific role for adipocyte SPHK1 in adipocyte function and inter-organ cross-talk that maintains overall metabolic homeostasis in obesity. Thus, SPHK1 serves a previously unidentified essential homeostatic role in adipocytes that protects from obesity-associated pathology.  These findings may have implications for pharmacological targeting of the SPHK1/S1P signaling axis.

**Supplementary key words** sphingosine-1-phosphate • sphingolipid • high-fat diet • obesity • metabolic disease • adipose • hepatocyte • lipotoxicity • cross-talk

This article contains [supplemental data](#).

<sup>†</sup>These authors contributed equally to this work.

\*For correspondence: L. Ashley Cowart, lauren.cowart@vcuhealth.org.

Obesity precipitates a variety of conditions, including type 2 diabetes, cardiovascular pathology, NAFLD, and others (1, 2). The molecular mechanisms connecting obesity to its downstream pathologies are not fully understood and are likely multi-faceted; however, data support major contributions from alterations in bioactive lipid metabolism and signaling. Among these, metabolism of sphingolipids, including ceramide and S1P, is altered in obese humans and in mouse models of obesity and contribute to obesity-induced pathology (3–6). Indeed, it is well-established that ceramide, a principal signaling sphingolipid, plays a role in insulin resistance (7–9). On the other hand, ceramide can be interconverted to S1P through the action of ceramidases and sphingosine kinases (SPHKs), SPHK1 and SPHK2. SPHK1 and its product, S1P, have also been identified as contributors to metabolic disease at least in part due to the well-documented pro-inflammatory signaling pathways through the S1P G protein-coupled receptors and downstream activation of NFκB signaling and other pathways of inflammation (5, 10, 11).

We and others have shown that SPHK1 and its product, S1P, are increased in several tissues in obese humans and mice, including liver, skeletal muscle, and adipose tissue (6, 12). We also showed that SPHK1 is induced by saturated fatty acids, which are elevated in the circulation of individuals with metabolic disease (6, 12). Therefore, because S1P is generally a pro-inflammatory lipid mediator, and because outcomes of obesity include systemic inflammation, this could serve as a primary mechanism by which lipid excess contributes to pathology. Supporting this, a previous study provided evidence that SPHK1 deficiency in mice was associated with enhanced insulin sensitivity and reduced pro-inflammatory signaling in adipose tissue of animals fed obesogenic diets (12). As adipose tissue inflammation is thought to be a key driver of obesity-related pathophysiology (13, 14), we speculated that SPHK1 expression in adipose tissue may mediate pro-inflammatory signaling, thereby promoting metabolic disease.

In this study, we generated a mouse strain lacking SPHK1 in adipose tissue (SK1<sup>fatKO</sup>). These animals were challenged

with HFD feeding for 18 weeks to assess the contribution of adipocyte SPHK1 to metabolic homeostasis, adipose tissue function, inflammation, and systemic glucose tolerance. In contrast to expected findings, mice exhibited components of metabolic phenotypes even on control diet (CD), and outcomes of high-fat feeding were exacerbated in these mice, including increased weight gain, impaired glucose clearance, and adipocyte hypertrophy. Adipocytes and adipose explants showed impaired lipolysis and dysregulation of lipolytic machinery. Moreover, the livers of these mice displayed NAFLD pathophysiology. Thus, SPHK1 serves a previously unidentified essential homeostatic role in adipocytes that protects from obesity-associated pathology. These data may have implications for pharmacological targeting of the SPHK1/S1P signaling axis.

## MATERIALS AND METHODS

### Generation of adipocyte-specific *Sphk1* KO mouse

Adipocyte-specific *Sphk1* KO mice (SK1<sup>fatKO</sup>) were generated by crossing B6;FVB-Tg(Adipoq-cre)1Evdrl/J (Jackson Laboratory strain 010803) and B6N.129S6-Sphk1<sup>tm2Cgh</sup>/J (Jackson Laboratory strain 019095) (15). Heterozygous mice were crossed to generate homozygous *flox/flox* or *+/+* breeding pairs. Genotype was confirmed using primers for the floxed *Sphk1* and adiponectin (*Adipoq*)-*Cre*. CRE-mediated homologous recombination removes exons 3–6 from the *Sphk1* gene (supplemental Fig. S1A). WT mice were all *Cre* carriers. Primers used for genotyping were as follows: *Cre1*, 5' ACGGACAGAAGCATTTTCCA 3'; *Cre2*, 5' GGAGTGC-CATGTGAGTCTG 3'; *Cre3*, 5' CTAGGCCACAGAATTGAAA-GATCT 3'; *Cre4*, 5' GTAGGTGGAAATTCTAGCATCATCC 3'; *Flox F*, 5' GGAACCTGGCTATGGAACC 3'; *Flox R1*, 5' ATGTTTCTTTC-GAGTGACC 3'; *Flox R2*, 5' AATGCCTACTGCTTACAAATACC 3'.

Gene depletion was confirmed by PCR amplification of a shortened fragment of the *Sphk1* gene in adipocyte genomic DNA from *flox/flox:Cre/Cre* mice, further described below and shown in supplemental Fig. S1.

### Animal model

All animal experiments conformed to the National Institutes of Health *Guide for the Care and Use of Laboratory Animals* and were in accordance with Public Health Service/National Institutes of Health guidelines for laboratory animal usage. The experimental groups consisted of male and female WT and SK1<sup>fatKO</sup> C57BL/6 mice. Mice were housed in the animal facility at the Medical University of South Carolina and Virginia Commonwealth University. Food and water were provided ad libitum, except when fasting was required (e.g., glucose tolerance testing). Animals were maintained on a 12:12 h light-dark cycle and ambient temperature was steadily 21°C. Animals were randomized to a high saturated fat diet (HFD) (Envigo, TD.09766) (60% kcal provided by milkfat) or an isocaloric low-fat diet (CD) (Envigo, TD.120455) (17% kcal provided by lard) at 6 weeks of age, and diets were administered for 18 weeks (n = 8–10 per group). On the day of euthanization, mice were fasted for 6 h and euthanized humanely by isoflurane (Hospira, Inc., Lake Forest, IL) followed by cardiac puncture. Cardiac blood was prepared for nonhemolyzed serum, aliquoted, and stored at –80°C until further analysis. Tissues were collected accordingly as fresh fixed in 10% neutral buffered formalin or fresh snap-frozen in liquid nitrogen and stored at –80°C until further processing. All experiments were performed under clean conditions, were approved by the Medical University of South

Carolina Institutional Animal Care and Use Committee, the Virginia Commonwealth University Institutional Animal Care and Use Committee, the Ralph H. Johnson Veterans Affairs Medical Center, and the Hunter Holmes McGuire Veterans Affairs Medical Center.

### Glucose tolerance test

Intraperitoneal glucose tolerance tests (ipGTTs) were performed on mice after 8 weeks of diet feeding (i.e., 14 weeks of age). Mice were fasted for 6 h before conducting a glucose tolerance test, generally 0830 to 1430. Mice received a sterile intraperitoneal injection of 2 mg/kg D-glucose. Blood was collected through a nick in the tail and analyzed neat using a One Touch UltraSmart blood glucose monitoring system at fasting for baseline blood glucose concentration and was then assessed 15, 30, 60, and 120 min after glucose injection.

### Bioplex

Serum cytokines (insulin, leptin) were measured using a multiplex adipokine assay service (Eve Biotechnologies).

### Triglyceride assay

Liver tissue homogenates were prepared according to the manufacturer's instructions with modifications (StanBio, 2200-225). Approximately 50 mg of liver tissue was homogenized in a 300  $\mu$ l solution of 2:1 100% ethanol and 30% potassium hydroxide, respectively. This was vortexed and allowed to incubate in a 60°C water bath for 5 h until the solution turned a translucent yellow with a visible pellet at the bottom. Then, 1.08 vol of 1 M MgCl<sub>2</sub> were added to the tube and vortexed to reach a milky consistency and left on ice for 10 min. Following this, tubes were vortexed and centrifuged for 30 min at 18,500 g at ambient temperature. The supernatant was collected, diluted 1:10 with PBS, and subjected to the triglyceride assay according to the manufacturer's instructions. In order to normalize to protein concentration by BCA, an aliquot is taken from the homogenate prior to water bath incubation, dried down, and resuspended in PBS. Ten microliters of sample and standards were assayed with 250  $\mu$ l of the triglyceride reagent. Water was used as a blank. Absorbances were read after 5 min incubation at 37°C at 500 nm.

### qPCR

Total RNA was isolated from gonadal adipose tissue and liver tissue homogenized in Trizol (Invitrogen, 15596026) followed by RNeasy mini kit (Qiagen, 74106) extraction and column purification. RNA integrity in tissue was assessed using the Agilent 2100 bioanalyzer by the Medical University of South Carolina Proteogenomics Facility. All RNA samples had RNA integrity number >7. cDNA was synthesized from 1  $\mu$ g of total RNA using iScript Advanced cDNA synthesis kit (Bio-Rad, 1708890). Real-time PCR was performed using a CFX96 Real-Time system (Bio-Rad) and SSoAdvanced Sybr (Bio-Rad, 1725272). The following primers were used: TATA box binding protein (*Tbp*) (Qiagen, PPM03560F), peptidylprolyl isomerase A (*Ppia*) (Qiagen, PPM03717B), and *Tnfr* (Qiagen, PPM03113G). Mean normalized expression was calculated by normalizing to the geometric mean of reference genes *Ppia* and *Tbp* in gonadal adipose tissue [i.e., root<sub>2</sub>(C<sub>q</sub> gene 1  $\times$  C<sub>q</sub> gene 2)] using the  $\Delta\Delta C_t$  method, where C<sub>q</sub> is the quantitation cycle and C<sub>t</sub> is the cycle threshold. Mean normalized expression was calculated using hydroxymethylbilane synthase 1 (*Hmbs1*) as the reference gene in liver tissue. Other primers were as follows: *Tbp*, forward (Fwd) 5' AAGGGAGAATCATGGACCAG 3', reverse (Rev) 5' CCGTAAGGCATCATTGGACT 3'; *Ppia*, Fwd 5' GAGCTGTTTGCAGACAAAGTTC 3', Rev 5' CCCTGGCACATGAATCCTGG 3'; *Hmbs1*, Fwd 5' ATGAGGGTGATTTCGAGTGGG 3',

Rev 5' TGTCTCCCGTGGTGGACATA 3'; *Adipoq*, Fwd 5' TGTTCCCTCTAATCCTGCCCA 3', Rev 5' CCAACCTGCACAAGTTCCCTT 3'; arginase 1 (*Arg1*), Fwd 5' TGGCTTGCAGACGTAGAC 3', Rev 5' GCTCAGGTGAATCGGCCTTTT 3'; diacylglycerol transferase 2 (*Dgat2*), Fwd 5' GAGGGTCTGGGCGATGGGCACT 3', Rev 5' CGACGGTGGTGATGGGCTTGGAGT 3'; *Fasn*, Fwd 5' GACTCGGCTACTGACACGAC 3', Rev 5' CGAGTTGAGCTGGGTTAGGG 3'; murine macrophage marker (also known as *Emr1*) (*F4/80*), Fwd 5' TCATGGCATACTGTTCACC 3', Rev 5' GAATGGGAGCTAAGGTCAAGTC 3'; interleukin-6 (*Il-6*), Fwd 5' TAGTCCTTCCCTACCCCAATTTCC 3', Rev 5' TTGTCCTTAGCCACTCCTTC 3'; *Leptin*, Fwd 5' CAAGCAGTGCATATCCAGA 3', Rev 5' AAGCCCAGGAATGAAGTCCA 3'; monocyte chemoattractant protein 1 (*Mcp1*), Fwd 5' TTAACAACTGATCGGAACCAA 3', Rev 5' GCATTAGCTTCAGATTTACGGGT 3'; *Sphk1*, Fwd 5' GAGTGCTGGTCTGCTGAA 3', Rev 5' AGGTATCTCTGCCTCCTCCA 3'; *Sphk2*, Fwd 5' CACGGCGAGTTTGTTTCCCTA 3', Rev 5' CTTCTGGCTTTGGGCGTAGT 3'; transforming growth factor- $\beta$ 1 (*Tgf $\beta$ 1*), Fwd 5' TGGCGTTACCTTGTAACC 3', Rev 5' GGTGTTGAGCCCTTTCCAG 3'.

### Basal lipolysis assay for NEFAs

Sera from mice and cell culture media containing only fatty acid-free BSA were prepared for NEFA assay according to the manufacturer's instructions (Wako Diagnostics; 999-34691, 995-34791, 991-34891, 993-35191, and 276-76491). Briefly, 5  $\mu$ l of sample (neat or diluted 1:10), calibrators, and blank were added in duplicate to a 96-well plate. Color reagent A solution (200  $\mu$ l) was added and incubated at 37°C for 5 min. Absorbance at 550 nm was acquired. Next, 100  $\mu$ l of color reagent B solution were added and incubated at 37°C for 5 min. Absorbance was read once more at 550 nm. After subtracting the blanks, the first reading was subtracted from the second reading to obtain the final absorbance, and concentrations were determined by standard curve normalization.

### Glycerol assay

The protocol was adapted from Sigma. Twenty-five microliters of cell culture media were assayed in duplicate in a 96-well plate. One hundred microliters of free glycerol reagent (Sigma, F6428) were added per well and incubated for 5 min at 37°C. Absorbance at 540 nm was measured on a spectrophotometer. Tissue explant glycerol release was normalized to tissue weight.

### Lipolysis in adipose tissue explants (ex vivo)

Gonadal adipose tissue was harvested from WT and SK1<sup>fatKO</sup> mice at 4–6 weeks of age. Tissue was cut into ~12 mg pieces. Two pieces were added to each well of a 12-well plate in 1 ml of DMEM/F12 + 1% fatty acid-free BSA and 1% antibiotic antimycotic solution (Sigma, A5955-100ML). Explants were incubated overnight at 37°C and 10% CO<sub>2</sub>. The next day, explants were transferred using forceps to new 12-well plates containing fresh media. Media were collected after 24 h for glycerol measurement.

### Histology and immunohistochemistry

Fresh liver tissue was snap-frozen in liquid nitrogen. 10- $\mu$ m Frozen sections (10  $\mu$ m) were prepared for measurement of hepatic neutral lipid accumulation by Oil Red O staining. Sections were counterstained with hematoxylin. Paraffin sections were prepared with adipose and liver tissue fixed in 10% neutral buffered formalin (1 h). Adipose sections were stained with H&E for adipocyte size analysis. Slides were imaged on a light microscope (Leica DMI1 microscope, Leica MCI70 HD camera), and a fluorescence microscope was only utilized for the adipose H&E adipocyte size quantification for better contrast with a 594 nm laser. In addition, imaging services were provided by the Virginia Commonwealth Uni-

versity Cancer Mouse Models Core using a brightfield whole-slide scanning Vectra Polaris (PerkinElmer) automated imaging system of H&E-stained gonadal white adipose tissue (gWAT) sections for assessment of crown-like structures (CLSs) using PhenoChart software (Akoya Biosciences, Marlborough, MA). For immunofluorescence histology, sections were subjected to antigen retrieval overnight at 60°C in 10 mM sodium citrate, 0.05% Tween 20 (pH 6.0) buffer. Slides were blocked using 5% donkey serum (host secondary antibody species). Slides were imaged on a Zeiss FV10i fluorescent microscope for myeloperoxidase (R&D Systems, AF3667, goat anti-mouse myeloperoxidase, 15  $\mu$ g/ml), a marker of infiltrating inflammatory immune cells. Secondary detection antibodies were from Life Technologies: Alexa 488 (Invitrogen, A-11055, donkey anti-goat IgG, 1:2,000) and ToPro3 to stain nuclei (Thermo Fisher, T3605, 1:2,000). Ten representative images per slide were analyzed by fluorescence intensity of puncta using ImageJ software (The National Institutes of Health, Bethesda, MD).

### Lipid measurements

Sphingolipids were measured using LC/MS/MS at the Virginia Commonwealth University Lipidomics and Metabolomics Core and performed using previously published methods (16, 17).

### Western blotting

Gonadal adipose tissue was homogenized in RIPA buffer with protease and phosphatase inhibitors (Thermo Fisher Scientific, 78446) using a Dounce homogenizer for at least 30 strokes, or until visibly homogenized. Homogenates were vortexed well and centrifuged at 10,000 *g* for 10 min at 4°C. The resulting infranant (below fat cake, and above cell debris pellet) was transferred to a new tube. Protein content was quantified using a BCA protein determination assay (Thermo Fisher Scientific, 23225). Homogenates were diluted 1:10 in RIPA with 2% SDS to minimize lipid interference in the BCA assay. Ten micrograms of protein were used for Western blotting. Nonhemolyzed mouse sera were diluted in PBS 1:20, and isovolumetric amounts of diluted sera plus loading buffer were loaded for Western blotting. gWAT proteins and sera proteins were separated by SDS-PAGE (Bio-Rad Criterion TGX stain-free precast gels) and transferred to PVDF membranes. The membranes were blocked for 1 h in 5% BSA. Proteins were detected using (gWAT) HRP-linked anti-rabbit secondary (Cell Signaling Technology, 7074, 1:5,000) or (sera) StarBright-700-linked anti-rabbit secondary (Bio-Rad, 12004161, 1:2,500), Clarity ECL Western blotting substrate (Bio-Rad, 1705061) for HRP, and a ChemiDoc imaging system (Bio-Rad, 17001401, 17001402). Blots were assessed for protein expression of ADIPOQ (Cell Signaling Technology, 2789, 1:2,000), adipose triglyceride lipase (ATGL) (Cell Signaling Technology, 2439, 1:2,000), abhydrolase domain containing 5 (ABHD5) (also known as CGI-58) (Novus Biologicals, NB100-5-7850, 1:1,000), and fatty acid binding protein 4 (FABP4) (Cell Signaling Technology, 2120, 1:2,000), vinculin (Cell Signaling Technology, 4650, 1:2,000), and stain-free total protein were used to determine even loading. Band intensity was quantified using ImageJ.

### Statistical analysis

All values are presented as mean  $\pm$  SEM. For single pairwise comparisons of normally distributed data sets, a Student's *t*-test was performed. For multiple comparisons of means, a one-way ANOVA with Tukey-Kramer post hoc test was performed. *P* < 0.05 was considered statistically significant. All hypothesis tests were conducted using GraphPad Prism 8 software. Experiments were performed in both male and female mice; data are shown by sex only where there were statistically significant differences between male and female experimental groups.

## RESULTS

Previous studies demonstrated that sphingosine kinase 1 (SPHK1) increased in adipose tissue of type 2 diabetic humans and in diet-induced obesity in mice (5). Moreover, in that study, global depletion of SPHK1 protected mice from HFD-induced insulin resistance and systemic inflammation. Because adipose tissue is a central regulator of metabolic homeostasis, and adipocyte dysfunction is thought to underlie much of the downstream pathophysiology of obesity, including insulin resistance and inflammation (14, 18), we sought to test the role of SPHK1 intrinsic to the adipocyte in these processes. To this end, mice with an adipocyte-specific deletion of SPHK1 (SK1<sup>fatKO</sup>) were generated using mice harboring a *Sphk1* allele with *Loxp* sites flanking exons 3–6. These mice were crossed with mice carrying a transgenic Cre recombinase enzyme driven by the Adipoq promoter (19). We confirmed gene depletion in the adipose tissue genomic DNA by PCR using an upstream primer 5' to exon 1 and a downstream primer 3' to exon 6, which should produce a 600 bp product only in the modified *Sphk1* gene. This product was indeed amplified and visualized by agarose gel (supplemental Fig. S1A, B), confirming gene depletion. Because SPHK1 depletion can be compensated by upregulation of SPHK2, mRNA for *Sphk2* was measured in gWAT homogenates of these mice (supplemental Fig. S1C). No upregulation of *SPHK2* was observed, indicating that this was not a confounding factor for data interpretation in these studies (supplemental Fig. S1C).

To test the effects of adipocyte-specific depletion of SPHK1 in pathophysiology in diet-induced obesity, SK1<sup>fatKO</sup> mice and their Adipoq-CRE:SK1<sup>+/+</sup> control counterparts were subjected to either a HFD or a control low glycemic isocaloric diet (CD) for 18 weeks. Mice on CD exhibited low levels of *Sphk1* mRNA (supplemental Fig. S1D). Adipose tissue homogenates from SK1<sup>fatKO</sup> mice exhibited some basal elevation of SPHK1; however, this was likely due to expression in other adipose tissue cell types. Similar to previous findings, HFD feeding robustly induced *Sphk1* mRNA in gWAT homogenates from control mice, and this was significantly attenuated in SK1<sup>fatKO</sup> mice, again, with residual message likely resulting from other adipose tissue cell types (e.g., immune cells, fibroblasts, vascular endothelial cells, etc.). SIP, the enzymatic product of SPHK1, was also very low in CD feeding but robustly induced by HFD feeding (supplemental Fig. S1E). While adipose tissue homogenates showed similar SIP levels in SK1<sup>fatKO</sup> mice and WT mice, SIP is found in micromolar amounts in plasma and even higher amounts in whole blood from erythrocytes (19–21), and therefore it is likely that these high levels obscured the differences in tissue SIP that would be expected based on reduced mRNA in the HFD-fed SK1<sup>fatKO</sup> mice. These data also suggest that SPHK1 in adipocytes does not contribute to circulating levels of SIP, but rather acts in a localized fashion within the tissue.

Previous studies indicated that, though *Sphk1*-null mice were protected from insulin resistance and inflammation induced by high-fat feeding, weight gain was comparable to that of control mice (5). In contrast, while HFD-feeding in-

creased weights of both SK1<sup>fatKO</sup> mice and control mice steadily over the first 8 weeks, by 8–10 weeks of the feeding course, SK1<sup>fatKO</sup> mice began to gain notably more weight on HFD compared with control (Fig. 1A). Indeed, by the end of the feeding course, the percent weight gain on CD and HFD was significantly greater in the SK1<sup>fatKO</sup> mice compared with the controls (Fig. 1B). Further analyses suggested that weight gain arose from expansion of both the gonadal (gWAT) and subcutaneous inguinal (iWAT) white adipose depots (Fig. 1C). On the other hand, retroperitoneal white adipose tissue (retroWAT) and intrascapular brown adipose tissue (BAT) depots did not exhibit such wet weight differences as gWAT and iWAT between genotypes (Fig. 1C). The remaining differences in weight between genotypes were most likely due to remaining subcutaneous fat (axial, gluteal, and other compartments beneath the skin) throughout the animal, which we observed in mutant animals upon dissection (data not shown). Therefore, in contrast to whole-body depletion of *Sphk1*, adipocyte-specific depletion exacerbated diet-induced obesity, suggesting a distinct role for adipocyte SPHK1 in inhibiting diet-induced obesity.

Though SK1<sup>fatKO</sup> mice were more obese than their control counterparts, obesity does not always coincide with metabolic disease (22), indicating a possibility for SK1<sup>fatKO</sup>, despite their increased adiposity, to be protected from deleterious metabolic outcomes of obesity, including impaired glucose clearing, a marker of insulin resistance. To test this, we performed glucose tolerance tests (GTTs). As expected, high-fat feeding impaired glucose clearing in control mice; however, these tests showed exacerbation of impaired glucose clearance in HFD-fed SK1<sup>fatKO</sup> mice compared with controls, both in kinetics of clearance and area under the curve (AUC) assessments (Fig. 1D, E). Fasting glucose was also elevated (Fig. 1F), and normalization of blood glucose in the GTT to basal glucose also demonstrated a significant elevation of AUC in CD- and HFD-fed SK1<sup>fatKO</sup> mice relative to control mice (supplemental Fig. S1F). Averaged fasting serum insulin trended strongly to increase in HFD-fed mutant mice relative to controls, and, though statistical significance was not reached ( $P = 0.1319$ , supplemental Fig. S1G), pairing fasting glucose with fasting insulin for each individual revealed a marked and significant increase in homeostatic model assessment of insulin resistance (HOMA-IR) in the HFD-fed SK1<sup>fatKO</sup> mice relative to controls (Fig. 1G). Together, these data support a role for adipocyte SPHK1 in suppressing HFD-induced obesity and subsequent deficiencies in glucose clearance.

Increased fat mass can arise from adipocyte hypertrophy (increase in cell size) and/or hyperplasia (increase in adipocyte number). While adipocyte hyperplasia may underlie the phenomenon of “healthy obesity” (i.e., WAT expansion with numerous smaller adipocytes and little inflammation or fibrosis), hypertrophic adipocytes more closely correlate to insulin resistance (23). Because the obese insulin-resistant phenotype was exacerbated in SK1<sup>fatKO</sup> mice, we hypothesized that they would show greater hypertrophy with high-fat feeding than controls. Upon histological examination, we found that the gonadal adipocytes in SK1<sup>fatKO</sup> mice were markedly larger than

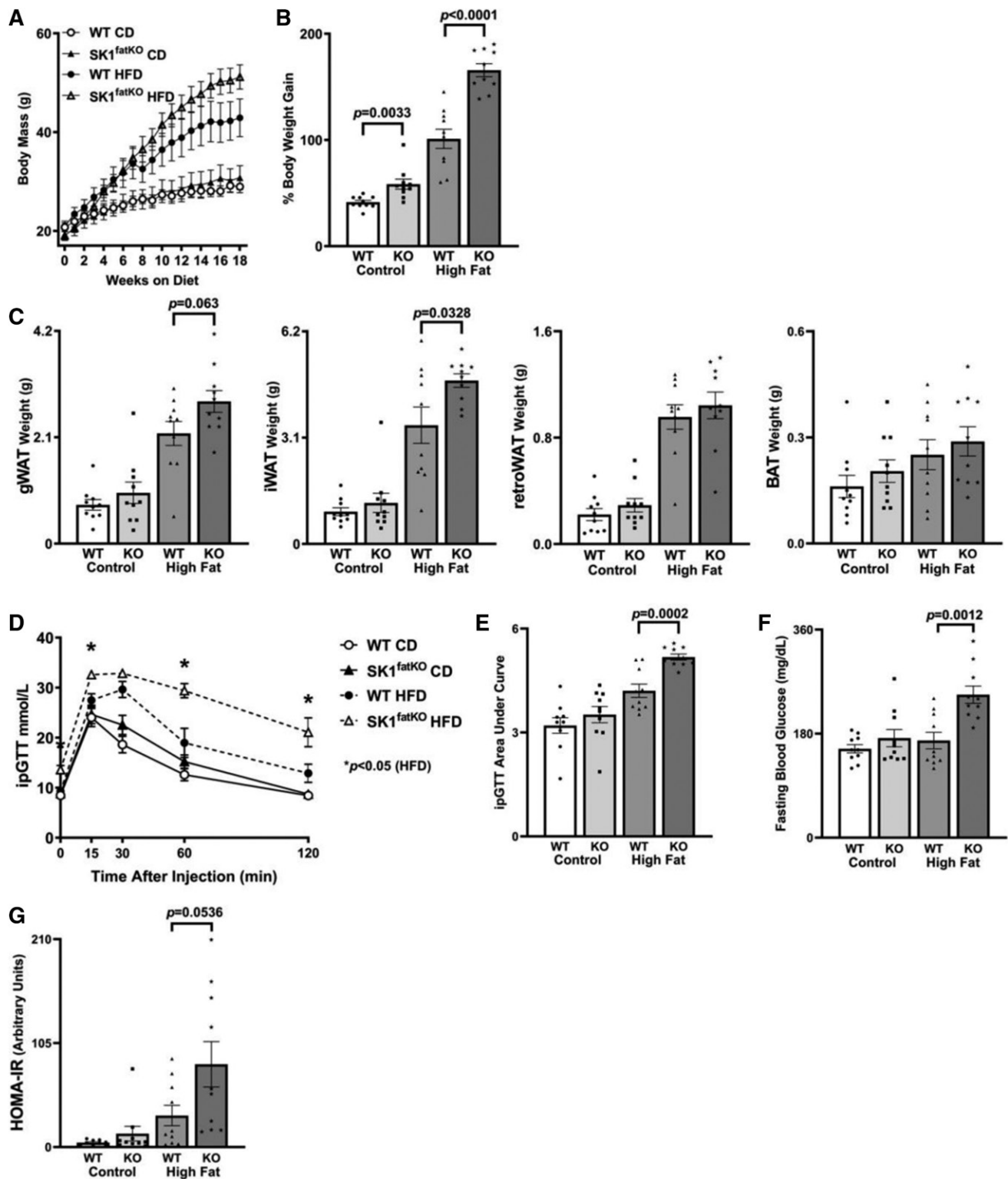


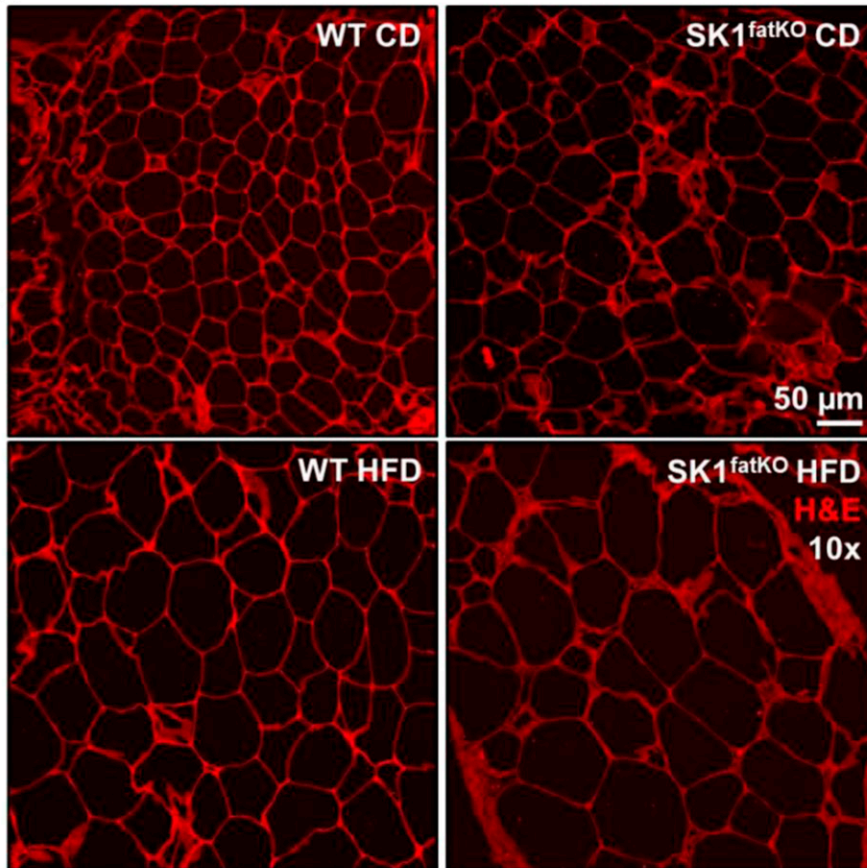
**Fig. 1.** HFD-induced weight gain and systemic glucose intolerance. **A:** Mouse body weights over 18 week HFD study. **B:** Percent weight gain between final weight at euthanization and initial starting weight at diet commencement. **C:** From left to right, gonadal (gWAT), subcutaneous (inguinal) fat pad (iWAT), retroperitoneal (retroWAT) fat pad, and brown adipose (BAT) weights at euthanization. **D:** After 18 weeks of high-fat feeding, an ipGTT was administered over 2 h, at the same time in the afternoon for each animal following a 6 h fast. **E:** The corresponding AUC analysis for ipGTT. **F:** Baseline fasting glucose shown as milligrams per deciliter as measured from whole tail blood droplets. **G:** HOMA-IR calculated from fasting blood glucose concentration and fasting blood insulin concentration.

those of control mice, even with CD feeding, and this was further increased with HFD feeding (Fig. 2A, B). Quantification of mean area showed an approximately 2-fold larger size in SK1<sup>fatKO</sup> on HFD relative to controls (Fig. 2C).

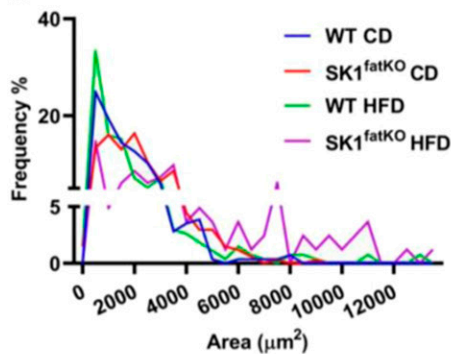
The hypertrophic adipocyte phenotype is generally considered to be more closely linked with overall metabolic perturbations and adipocyte dysfunction, and, therefore, the larger adipocytes observed in SK1<sup>fatKO</sup> mice suggested that there could be a general disruption of key adipocyte functions. The endocrine function of adipose tissue is essential for metabolic homeostasis, and aberrant adipokine production and signaling is a key feature of obesity-induced meta-

bolic disease and closely associated with adipocyte size (14). For example, hyperleptinemia and leptin resistance occur in human obesity and mouse models, and leptin secretion by human adipocytes correlated directly with adipocyte size (24). Consistent with this, HFD increased leptin mRNA in SK1<sup>fatKO</sup> mice to a greater extent than in control mice (Fig. 2D). Serum leptin trended modestly higher in SK1<sup>fatKO</sup> mice upon HFD feeding; however, this did not meet criteria for statistical significance (supplemental Fig. S2A). ADIPOQ, produced by adipocytes, is a protective factor in the context of metabolic disease and acts on multiple cell types and tissues for anti-atherogenic and anti-diabetic effects.

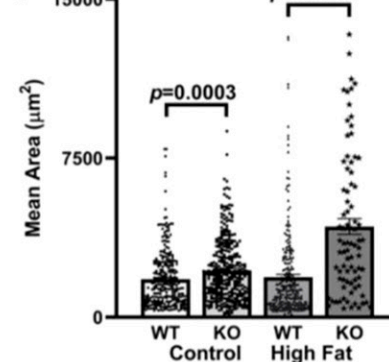
**A**



**B**



**C**



**D**

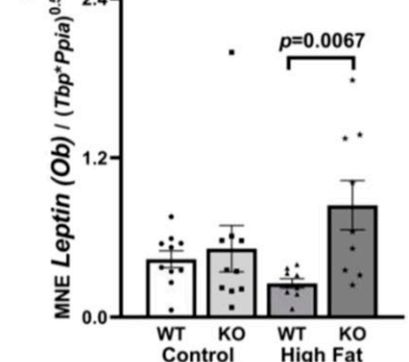


**Fig. 2.** Adipocyte hypertrophy in SK1<sup>fatKO</sup> gWAT. **A:** Confocal microscopy of representative sections of gWAT shown by H&E staining. **B:** Quantification of gWAT adipocyte size, as shown by a frequency distribution. **C:** Adipocyte size displayed as the mean  $\pm$  SEM. **D:** Pro-inflammatory adipokine *leptin* (*Ob*) mRNA expression in gWAT.

ADIPOQ production is decreased in obesity and inversely correlated with adipocyte hypertrophy. *Adipoq* mRNA from adipose tissue homogenates was modestly reduced in SK1<sup>fatKO</sup> mice on CD, consistent with larger basal adipocytes; however, no differences were observed between SK1<sup>fatKO</sup> and control mice on HFD (supplemental Fig. S2B). In mouse sera, ADIPOQ levels were higher in female mice generally, but showed no differences by diet or genotype. In males, however, high-fat feeding reduced circulating ADIPOQ by 50% (supplemental Fig. S2C). Notwithstanding, significant sex differences were not observed in other measures, suggesting that decreased ADIPOQ could not explain the robust exacerbation in insulin resistance observed in both male and female SK1<sup>fatKO</sup> mice. ADIPOQ receptors (highly expressed in the liver) are thought to have intrinsic ceramidase activity (25). Liver ceramides and hexosylceramides were measured among groups, which indicated that, while no major effects were observed in the HFD-fed condition, low glycemic CD-fed SK1<sup>fatKO</sup> mice had increased C22:0 and C:24 ceramides and decreased C18:0 and C22:0 hexosylceramides in their livers (supplemental Fig. S2D, E).

Inflammation in gWAT is closely associated with adipocyte hypertrophy and is thought to couple obesity to insulin resistance (13, 26–28). Moreover, a previous study showed that SPHK1-null mice were protected from inflammation upon high-fat feeding (5). Inflammation in gWAT was assessed by several markers. First, mRNA of macrophage marker F4/80 was measured, and data showed that expression was similar in both WT and SK1<sup>fatKO</sup> mice on CD, though there was a trend to increase in HFD-fed mutant mice relative to control mice on HFD (Fig. 3A). Consistent with this, the macrophage chemoattractant protein marker, *Mcp1*, increased by HFD-feeding in both strains but was not significantly different between strains (Fig. 3B). CLSs in gWAT were identified, and negligible differences in numbers were found between genotypes, although CLSs tended to be less frequent in females compared with males (Fig. 3C, and data not shown). Partially consistent with previous work showing protection from pro-inflammatory cytokine expression in obesity in SPHK1-null mice, HFD-fed SK1<sup>fatKO</sup> mice showed strong trends toward decreased *Il-6* and *Tnfa* levels, though these did not reach statistical significance (Fig. 3D, E). As F4/80 does not necessarily indicate macrophage polarization status (e.g., M1 vs. M2), M2 macrophage markers were also assessed. *Arg1* showed no changes (Fig. 3F); however, there was a pronounced increase of *Tgfb1* in SK1<sup>fatKO</sup> mice on HFD (Fig. 3G). Assessment of neutrophil infiltration by myeloperoxidase puncta visualization and quantification showed little if any difference between WT and SK1<sup>fatKO</sup> mice (supplemental Fig. S3A, B). In summary, relative to HFD-fed control mice, SK1<sup>fatKO</sup> mice showed more fat mass, exacerbated glucose intolerance, and basal adipocyte hypertrophy, which was exaggerated upon high-fat feeding. However, while adipocyte hypertrophy is linked to inflammation and impaired adipokine production, increases in these measures in the gWAT of SK1<sup>fatKO</sup> relative to control mice were modest, at best, and largely negligible, suggesting other links between adipocyte-specific depletion of SPHK1, obesity, and impaired glucose clearance.

Other than endocrine function, adipocytes perform lipogenesis and lipolysis to contribute to metabolic homeostasis. Therefore, we hypothesized that SPHK1 may play a role in regulating these processes. Lipolysis increases with fasting to release FFAs into circulation where they can be distributed to peripheral organs and tissues for energy production in the context of low glucose (29). To test whether lipolysis may be impaired in SK1<sup>fatKO</sup> mice, we assessed serum NEFA in fasted HFD-fed mice. These data demonstrated a 20–25% reduction in serum NEFA in HFD-fed SK1<sup>fatKO</sup> mice (Fig. 4A). To test whether this was due to deficient adipose tissue lipolysis, glycerol release of explants of gWAT from SK1<sup>fatKO</sup> mice was measured. Consistent with decreased fasting NEFA observed in vivo, explants from mutant mice released only ~50% of the glycerol released by explants of control mice (Fig. 4B). These differences were only observed in basal lipolysis, as isoproterenol-stimulated lipolysis showed no differences between WT and mutant cells (data not shown). Consistent with this, critical mediators of adipocyte lipolysis, including ATGL, CGI-58, and FABP4, were all lower in SK1<sup>fatKO</sup> mice at basal and/or HFD-fed conditions (Fig. 4C, D). In general, levels of these were lower in mutant mice, with females showing statistically significant differences and males mirroring this trend (Fig. 4D, densitometry values shown in supplemental Table S1). Therefore, adipocyte SPHK1 plays a role in basal lipolysis and likely contributes to fasting circulating NEFA.

Adipocyte hypertrophy and impaired function arise when adipocytes reach their capacity for lipid storage, at which point ectopic lipid deposition occurs in other organs and tissues including liver (30). Thus, livers in SK1<sup>fatKO</sup> mice were tested for pathology consistent with NAFLD. HFD-fed SK1<sup>fatKO</sup> mice showed an over 2-fold increase in liver triacylglycerol (TAG) relative to control mice fed HFD (Fig. 5A), and this was consistent with Oil Red O staining of neutral lipid, which showed increased lipid and also that both male and female mice exhibited macrosteatosis (Fig. 5B). Liver steatosis can arise from several mechanisms, including increased lipid uptake, decreased lipid secretion, or increased lipogenesis. Because serum NEFAs were lower in SK1<sup>fatKO</sup> mice, increased uptake seemed an unlikely mechanism. However, lipogenic machinery *Fasn* and *Dgat2* mRNA were significantly elevated on CD and/or HFD (Fig. 5C, D). In addition to steatosis, further evidence of progression of NAFLD included *Mcp1* and *Tnfa* increase in HFD-fed SK1<sup>fatKO</sup> mice (Fig. 5E, F). Fibrogenic activity was suggested by elevated collagen type I alpha 1 chain (*Col1a1*) mRNA, which increased in male mutant mice (Fig. 5G). Data were separated by sex to illustrate that male mice more strongly exhibited the effects of liver fibrosis than female mice, who showed no significant increase. This is consistent with data showing that females of reproductive age exhibit less fibrosis in NAFLD (31).

## DISCUSSION

Previous data from our laboratory and others indicated that SPHK1 was involved in pathological mechanisms related to metabolism in various tissues, including adipose,

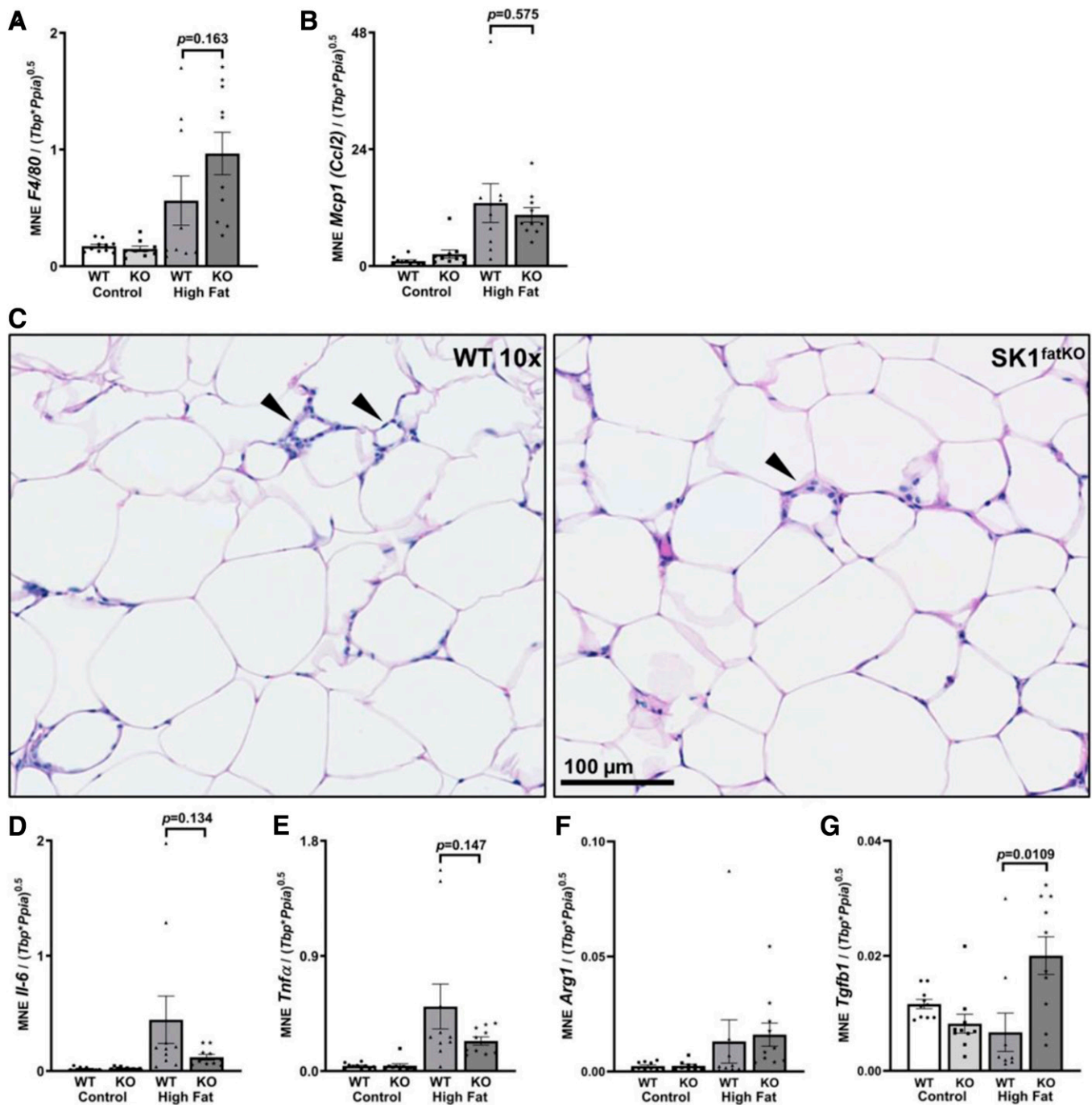


**Fig. 3.** Inflammation within the adipose tissue. mRNA was isolated from gWAT homogenates from mice of both genotypes on both diets. After cDNA preparation, real-time PCR was used to measure message for the indicated proteins A: Inflammatory adipocytokine *F4/80* (*Emr1*). B: Pro-inflammatory M1 macrophage *Mcp1* [C-C motif chemokine ligand 2 (*Ccl2*)]. C: Representative CLSs shown by brightfield H&E in gWAT from HFD-fed mice (black arrowheads). D: Pro-inflammatory *Il-6* transcript. E: Pro-inflammatory *Tnf $\alpha$*  transcript. F: M2 macrophage marker *Arg1*. G: M2 macrophage marker *Tgfb1*.

muscle, liver, and pancreas (2, 6, 12, 32). Furthermore, previous studies have shown that constitutive deletion of SPHK1 elicits protection from HFD-induced diabetes and inflammation (5). Given the importance of adipose tissue function on whole-body metabolism and its role in the development of the metabolic syndrome, our goal in this study was to determine whether adipocyte SPHK1/S1P plays a specific role in pathophysiology associated with obesity. Specifically, as S1P is largely a pro-inflammatory lipid mediator, and adi-

pose tissue inflammation occurs in obesity and is thought to underlie maladaptive responses to obesity, we hypothesized that depletion of adipocyte SPHK1 would be protective in the obese context. Surprisingly, however, physiological characterization of SK1<sup>fatKO</sup> mice revealed that SPHK1 depletion from adipocytes exacerbated outcomes of diet-induced obesity in mice. Specifically, SK1<sup>fatKO</sup> mice gained more weight, had hypertrophic adipocytes, and had decreased glucose tolerance relative to controls, and they exhibited liver



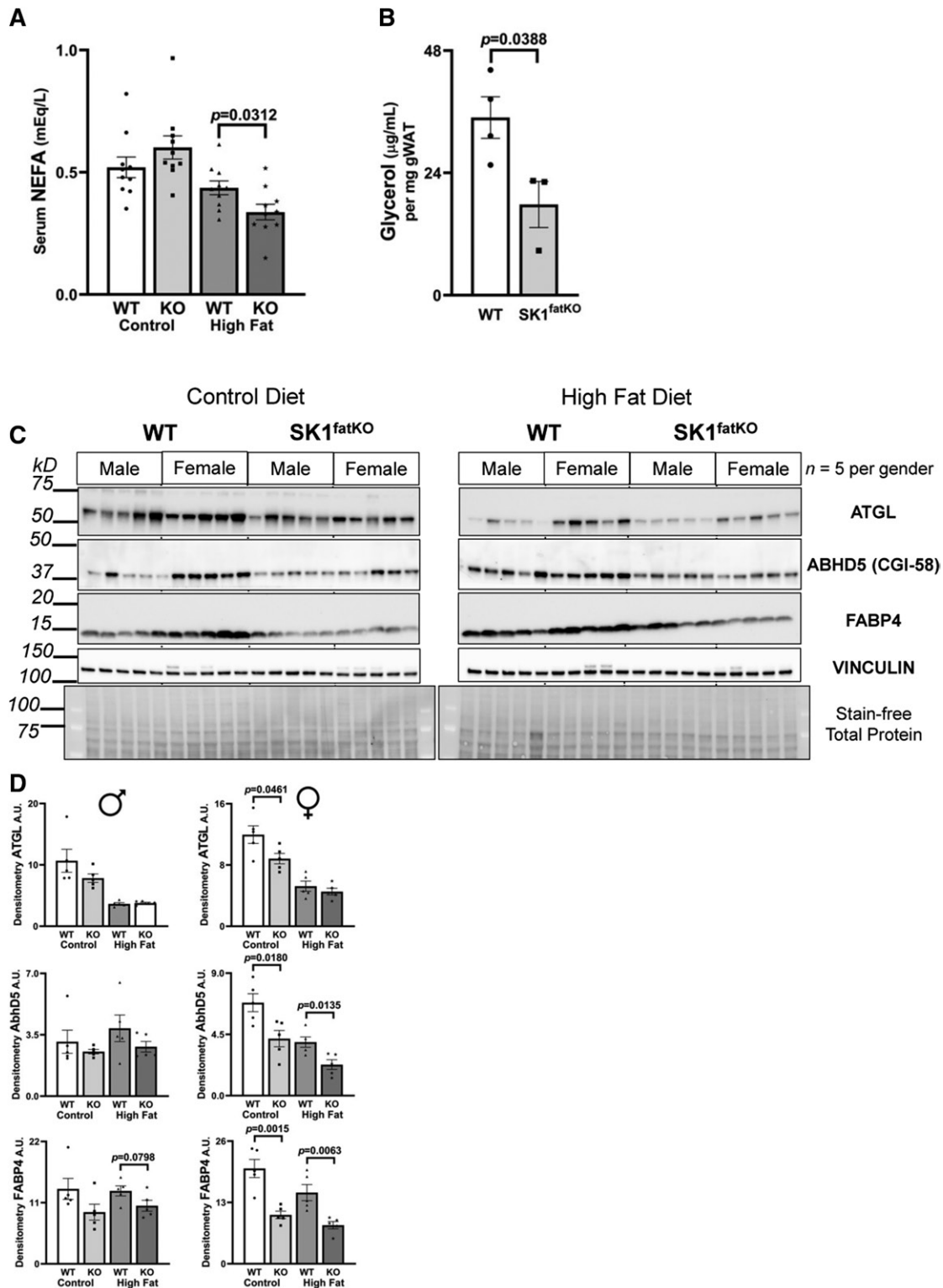


**Fig. 4.** Fasting serum NEFA, basal glycerol release, and lipolytic proteins are reduced in  $SK1^{fatKO}$  mice. A: Serum NEFAs were measured from mice fasted for 6 h. B: gWAT explants were incubated in fatty acid-free medium for 48 h and medium glycerol was measured. Medium glycerol was normalized to the weight of tissue utilized in each well. C: Western blot protein analysis of lipolytic proteins (ATGL, CGI-58, FABP4) from gWAT. Protein loading was normalized by stain-free total loading, as well as vinculin. D: Band intensities were quantified by densitometry using ImageJ and graphed separated by sex (males on left, females on right) showing mean  $\pm$  SEM.

steatosis and inflammation indicative of a NASH phenotype. These findings suggest that adipocyte SPHK1 is required for normal systemic metabolic homeostasis and also can at least partially attenuate some negative outcomes of obesity.

As the product of SPHK1, S1P is an established immune cell chemoattractant; we were surprised to see little impact of SPHK1 depletion on adipose tissue inflammatory markers in HFD-fed mice. Though two key indicators of an

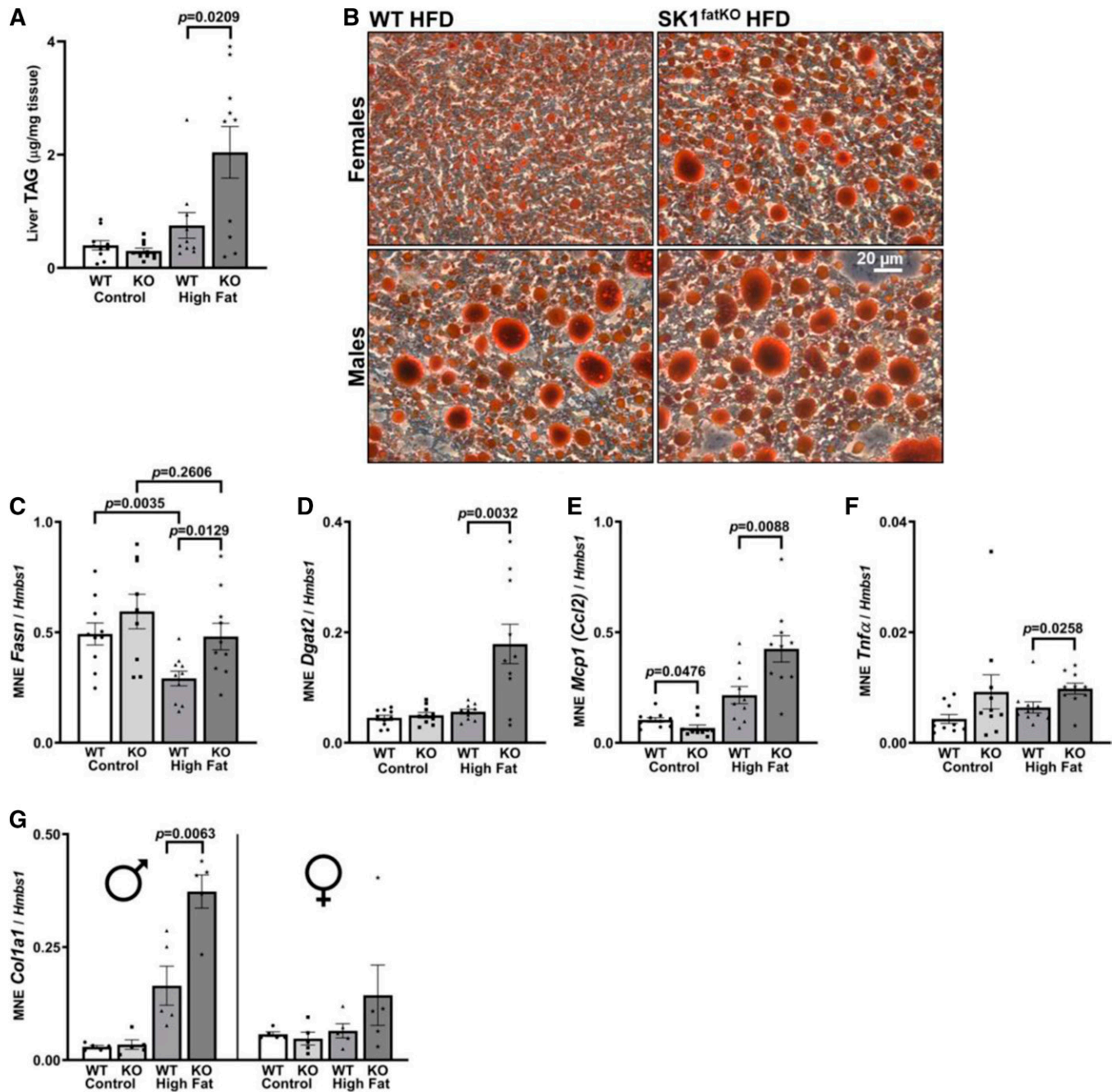


**Fig. 5.** Serum TAG, liver lipid accumulation, and lipogenesis. **A:** Total liver TAGs. **B:** Oil Red O-stained sections in HFD condition separated by sex. **C:** Liver lipogenic gene expression of *Fasn*. **D:** Liver lipogenic gene expression of *Dgat2*. **E:** Liver pro-inflammatory cytokine marker *Mcp1*. **F:** Liver pro-inflammatory cytokine marker *Tnf $\alpha$*  mRNA expression. **G:** Liver fibrotic gene expression of *Col1a1* separated by sex, males on left, females on right.

inflammatory phenotype, *Tnf $\alpha$*  and IL-6, showed a trend toward decrease in SK1<sup>fatKO</sup> mice on HFD relative to controls on HFD, these measures did not reach statistical significance. Additionally, neutrophil infiltration, previously shown to be influenced by the SIP signaling axis in liver (33), was not notably different in adipose tissue between genotypes in this study. As yet undiscovered outcomes of SPHK1 depletion in adipocytes therefore must outweigh the potential protection from inflammation. This is intriguing, as adipose tissue inflammation is thought to be a central link between obesity and insulin resistance. Therefore,

as these animals had an exacerbated metabolic phenotype with no increase in inflammation, this study essentially decouples adipose tissue inflammation from insulin resistance. This also indicates that the protection from adipose tissue inflammation in obesity as previously observed in the constitutive SPHK1-null mouse arose from SPHK1 in other cell types and not adipocytes. Therefore, our findings suggest that SPHK1 has homeostatic roles in adipocytes in the obese context, an idea that has not been appreciated before.

While molecular mechanisms by which SPHK1 regulates adipocyte function and resulting metabolic homeostasis

are not clear, some findings from this study may shed light on the roles of adipocyte SPHK1 in obesity. First, decreased lipolytic enzymes were observed in SKI<sup>fatKO</sup> mice, consistent with lower fasting NEFAs, lower glycerol release of explants, and larger adipocytes. This suggests a fundamental role for SPHK1 in facilitating lipolysis in obesity; as unrestrained lipolysis elevates NEFAs in metabolic disease, and because SPHK1 animals had reduced NEFAs, this might present a strategy for modulation of circulating lipids.

Second, TGF- $\beta$ 1 was much higher in SKI<sup>fatKO</sup> adipose tissue homogenates on HFD than that of control mice on HFD. TGF- $\beta$ 1 is largely anti-adipogenic and promotes adipocyte dedifferentiation (34), which could potentially underlie the hypertrophic adipocyte phenotype. This idea is supported by findings that deletion of SMAD3, a downstream signaling effector of TGF- $\beta$ 1, decreased adipocyte size (35). Numerous studies across a variety of experimental contexts place TGF- $\beta$  upstream of SPHK1, especially in the context of fibrosis (36, 37); our results suggest that SPHK1 negatively regulates TGF- $\beta$ , which not only presents an additional relationship between the SPHK1 and TGF- $\beta$  axis but also suggests a negative feedback loop that is potentially important in adipocyte regulation.

Third, adipocyte hypertrophy is strongly associated with adipose tissue inflammation, which is thought to contribute to systemic insulin resistance in obesity (14, 38). However, as previously discussed, SKI<sup>fatKO</sup> mice had little if any differences in HFD-induced gWAT inflammatory markers, which actually trended toward a decrease relative to control mice. This suggests that, though SPHK1 may mediate inflammation downstream of adipocyte hypertrophy, a beneficial role of SPHK1 in regulating adipocyte size and lipolysis is supported by our findings here, suggesting dual and opposing roles for adipocyte SPHK1 in obesity.


Despite lowered trends in lipolysis, mutant mice were still highly glucose intolerant and heavier compared with their control counterparts (Fig. 1A, B, D). This finding stands in contrast to other lipolysis-deficient models, such as *Atgl* KO mice, which have vastly different body temperatures and drastic ectopic cardiac lipid deposition compared with control mice, whereas we did not observe such changes (data not shown) (39). Furthermore, in a model of pharmacological inhibition of lipolysis, in which mice were treated with the compound Atglistatin, adipocyte size was decreased and body weight was significantly lowered compared with untreated mice, which also contrasts to the greater weight gain and adipocyte hypertrophy we observed in SKI<sup>fatKO</sup> animals (Figs. 1A, B; 3C) (40). These apparent discrepancies suggest that, though lowering ATGL may protect from pathology associated with obesity, other effects of SPHK1 depletion outweigh any potential protection. Furthermore, combined with the effects on ABHD5 and FABP4, this may indicate an overall lesser ability to perform lipolysis in adipose tissue from mutant mice (Fig. 4C, D). Intriguingly, ATGL-null mice do not exhibit differences in basal adipose glycerol release compared with control mice, suggesting that other lipases contribute to lipolytic products secreted from the tissue (39). This could include other players such as (G0S2), fat-specific protein

27 (FSP27), hypoxia inducible lipid droplet-associated protein (HILPDA), and/or patatin-like phospholipase domain-containing protein 3 (PNPLA3) (which were not assessed here) (41, 42).

In this study we adhered to recent imperatives to study both sexes. In general, data were similar between male and female animals. In some instances, trends were the same and statistically significant within each sex, but combining sexes led to greater variation and therefore higher *P*-values. In cases where data from each sex would lead to different conclusions, data were presented separately for male and female animals. For example, serum levels of ADIPOQ, an insulin-sensitizing adipokine that is largely beneficial in the metabolic context, were lower in male mice. On the other hand, liver *Colla1* expression was higher in male mice. In general, these findings agree with current literature on sex differences in cardiometabolic disease. Additionally, because the major phenotypes described did not differ between sexes (e.g., decreased glucose tolerance, adipocyte hypertrophy, *Tgf- $\beta$ 1* expression on HFD, etc.), parameters that were distinct between sexes do not likely underlie the common phenotypes. For some investigators, however, these differences may be of interest.

While inter-organ cross-talk in obesity is of increasing interest, the mechanism(s) by which SPHK1 depletion in adipocytes causes NAFLD symptoms are not understood. Normally, the liver serves as a short-term reservoir for excess circulating lipid from the diet and adipose tissue lipolysis, along with lipids generated by the liver through de novo lipogenesis. NAFLD progresses as lipid supply exceeds the rate at which the liver can utilize or export it. Impairments of glucose signaling and adipose tissue expansion, along with adipose inflammation and toxic lipid overload all contribute to the development of steatosis. NAFLD progression is multifaceted and it is increasingly evident that adipose tissue impairment is directly involved, but these mechanisms are not fully defined (43). We show elevation of machinery for de novo lipogenesis, which may explain simple steatosis in the liver; however, mechanisms by which this could occur from ablation of SPHK1 in adipocytes will require further study to uncover. A recent study suggested that extracellular vesicles from adipocytes could deliver TGF- $\beta$ 1 to hepatocytes, where it is pro-fibrotic (44). Indeed, we observed increased *Tgf- $\beta$ 1* in adipocytes and increased expression of *Colla1* in liver in SKI<sup>fatKO</sup> animals on HFD. While reduced glucose tolerance and adipose expandability are likely contributors to the steatosis observed in HFD-fed SKI<sup>fatKO</sup> mice, further studies will be required to determine mechanisms mediating SPHK1-dependent adipocyte-liver cross-talk.

In conclusion, as SPHK1 generates S1P, a pro-inflammatory lipid mediator, and its global depletion protected from numerous metabolic phenotypes in diet-induced obesity in mice, we hypothesized that its depletion in adipocytes would also protect from pathological outcomes associated with high fat feeding. However, we found that adipocyte-specific depletion of SPHK1 led to exacerbated glucose intolerance, adipocyte hypertrophy, and impaired lipolysis, supporting a beneficial role for SPHK1 in adipocytes

in the obese context. In addition to revealing novel functions of SPHK1 in adipocytes, our findings may have implications for targeting the SPHK/SIP axis for therapeutic advantage in multiple contexts. 

#### Acknowledgments

The authors would like to acknowledge discussions with Drs. Rana Gupta and Lavanya Vishvanath at the Touchstone Diabetes Center at the University of Texas Southwestern for essential discussions on adipocyte culture and differentiation and on adipose tissue biology. Services in support of the research project were provided by the Virginia Commonwealth University Lipidomics/Metabolomics Core, supported, in part, with funding from the National Institutes of Health-National Cancer Institute Cancer Center Support Grant, as well as a shared resource grant S10-RR-031535 from the National Institutes of Health. Grant P30 CA016059 to the Virginia Commonwealth University Massey Cancer Center also supported services essential to this work including the Microscopy Shared Resource and the Virginia Commonwealth University Massey Cancer Center Cancer Mouse Model Shared Resource.

#### Author contributions

A.K.A, J.M.L, and L.A.C. designed experiments; A.K.A, J.M.L, D.J.M., B.N.T., and P.R. performed experiments and analyzed data; W.L.H. provided critical intellectual input; A.K.A, J.M.L, and L.A.C. wrote the manuscript.

#### Author ORCIDs

L. Ashley Cowart  <https://orcid.org/0000-0002-5312-5232>

#### Funding and additional information

This work was supported by US Department of Veterans Affairs Merit Award 2I0BX000200 and National Institutes of Health Grants 1R01HL117233 and 1R01HL151243 (L.A.C.). Additional support was provided by Cell and Molecular Imaging Shared Resource Center, Hollings Cancer Center, Medical University of South Carolina Grant S10-OD-018113; the Medical University of South Carolina Proteogenomics Facility; and the Medical University of South Carolina Histology and Immunohistochemistry Laboratory. The content is solely the responsibility of the authors and does not necessarily represent the official views of the National Institutes of Health.

#### Conflict of interest

The authors declare that they have no conflicts of interest with the contents of this article.

#### Abbreviations

ABHD5, abhydrolase domain containing 5 also known as (CGI-58); Adipoq, adiponectin; Arg1, arginase 1; ATGL, adipose triglyceride lipase; AUC, area under the curve; BAT, brown adipose tissue; CD, control diet; CGI-58, lipid droplet binding protein (also known as ABHD5); CLS, crown-like structure; Coll1a1, collagen type I alpha 1 chain; Dgat2, diacylglycerol transferase 2; Emr1, EGF-like module-containing mucin-like hormone receptor-like 1; F4/80, murine macrophage marker (also known as Emr1); FABP4, fatty acid binding protein 4; Fwd, forward; GTT, glucose tolerance test; gWAT, gonadal white

adipose tissue; HOMA-IR, homeostatic model assessment of insulin resistance; Il-6, interleukin-6; ipGTT, intraperitoneal glucose tolerance test; iWAT, inguinal white adipose tissue; Mcp1, monocyte chemoattractant protein 1; Ppia, peptidylprolyl isomerase A; retroWAT, retroperitoneal white adipose tissue; Rev, reverse; SKI<sup>fatKO</sup>, Sphk1<sup>fl/fl</sup>:adiponectin-Cre; SPHK, sphingosine kinase; TAG, triacylglycerol; Tbp, TATA box binding protein; Tgf-β1, transforming growth factor-β1.

Manuscript received April 30, 2020, and in revised form June 29, 2020. Published, JLR Papers in Press, July 20, 2020, DOI 10.1194/jlr.RA120000875.

## REFERENCES

1. Dal Canto, E., A. Ceriello, L. Ryden, M. Ferrini, T. B. Hansen, O. Schnell, E. Standl, and J. W. Beulens. 2019. Diabetes as a cardiovascular risk factor: an overview of global trends of macro and micro vascular complications. *Eur. J. Prev. Cardiol.* **26**: 25–32.
2. Aguilar-Salinas, C. A., and T. Viveros-Ruiz. 2019. Recent advances in managing/understanding the metabolic syndrome. *F1000 Res.* **8**: doi:10.12688/f1000research.17122.1.
3. Hannun, Y. A., and L. M. Obeid. 2018. Sphingolipids and their metabolism in physiology and disease. *Nat. Rev. Mol. Cell Biol.* **19**: 175–191.
4. Choi, S., and A. J. Snider. 2015. Sphingolipids in high fat diet and obesity-related diseases. *Mediators Inflamm.* **2015**: 520618.
5. Wang, J., L. Badeanlou, J. D. Bielawski, T. P. Ciaraldi, and F. Samad. 2014. Sphingosine kinase 1 regulates adipose proinflammatory responses and insulin resistance. *Am. J. Physiol. Endocrinol. Metab.* **306**: E756–E768.
6. Geng, T., A. Sutter, M. D. Harland, B. A. Law, J. S. Ross, D. Lewin, A. Palanisamy, S. B. Russo, K. D. Chavin, and L. A. Cowart. 2015. SphK1 mediates hepatic inflammation in a mouse model of NASH induced by high saturated fat feeding and initiates proinflammatory signaling in hepatocytes. *J. Lipid Res.* **56**: 2359–2371.
7. Chavez, J. A., T. A. Knotts, L.-P. Wang, G. Li, R. T. Dobrowsky, G. L. Florant, and S. A. Summers. 2003. A role for ceramide, but not diacylglycerol, in the antagonism of insulin signal transduction by saturated fatty acids. *J. Biol. Chem.* **278**: 10297–10303.
8. Chavez, J. A., and S. A. Summers. 2012. A ceramide-centric view of insulin resistance. *Cell Metab.* **15**: 585–594.
9. Cowart, L. A. 2009. Sphingolipids: players in the pathology of metabolic disease. *Trends Endocrinol. Metab.* **20**: 34–42.
10. Lee, S. Y., I. K. Hong, B. R. Kim, S. M. Shim, J. Sung Lee, H. Y. Lee, C. Soo Choi, B. K. Kim, and T. S. Park. 2015. Activation of sphingosine kinase 2 by endoplasmic reticulum stress ameliorates hepatic steatosis and insulin resistance in mice. *Hepatology.* **62**: 135–146.
11. Japtok, L., E. I. Schmitz, S. Fayyaz, S. Krämer, L. J. Hsu, and B. Kleuser. 2015. Sphingosine 1-phosphate counteracts insulin signaling in pancreatic β-cells via the sphingosine 1-phosphate receptor subtype 2. *FASEB J.* **29**: 3357–3369.
12. Ross, J. S., W. Hu, B. Rosen, A. J. Snider, L. M. Obeid, and L. A. Cowart. 2013. Sphingosine kinase 1 is regulated by peroxisome proliferator-activated receptor α in response to free fatty acids and is essential for skeletal muscle interleukin-6 production and signaling in diet-induced obesity. *J. Biol. Chem.* **288**: 22193–22206.
13. Gustafson, B., A. Hammarstedt, C. X. Andersson, and U. Smith. 2007. Inflamed adipose tissue: a culprit underlying the metabolic syndrome and atherosclerosis. *Arterioscler. Thromb. Vasc. Biol.* **27**: 2276–2283.
14. Scherer, P. E. 2006. Adipose tissue: from lipid storage compartment to endocrine organ. *Diabetes.* **55**: 1537–1545.
15. Pappu, R., S. R. Schwab, I. Cornelissen, J. P. Pereira, J. B. Regard, Y. Xu, E. Camerer, Y.-W. Zheng, Y. Huang, and J. G. Cyster. 2007. Promotion of lymphocyte egress into blood and lymph by distinct sources of sphingosine-1-phosphate. *Science.* **316**: 295–298.
16. Haynes, C. A., J. C. Allegood, H. Park, and M. C. Sullards. 2009. Sphingolipidomics: methods for the comprehensive analysis of sphingolipids. *J. Chromatogr. B Analyt. Technol. Biomed. Life Sci.* **877**: 2696–2708.

17. Shaner, R. L., J. C. Allegood, H. Park, E. Wang, S. Kelly, C. A. Haynes, M. C. Sullards, and A. H. Merrill, Jr. 2009. Quantitative analysis of sphingolipids for lipidomics using triple quadrupole and quadrupole linear ion trap mass spectrometers. *J. Lipid Res.* **50**: 1692–1707.
18. Kusminski, C. M., P. E. Bickel, and P. E. Scherer. 2016. Targeting adipose tissue in the treatment of obesity-associated diabetes. *Nat. Rev. Drug Discov.* **15**: 639–660.
19. Allende, M. L., T. Sasaki, H. Kawai, A. Olivera, Y. Mi, G. van Echten-Deckert, R. Hajdu, M. Rosenbach, C. A. Keohane, and S. Mandala. 2004. Mice deficient in sphingosine kinase 1 are rendered lymphopenic by FTY720. *J. Biol. Chem.* **279**: 52487–52492.
20. Yatomi, Y., Y. Igarashi, L. Yang, N. Hisano, R. Qi, N. Asazuma, K. Satoh, Y. Ozaki, and S. Kume. 1997. Sphingosine 1-phosphate, a bioactive sphingolipid abundantly stored in platelets, is a normal constituent of human plasma and serum. *J. Biochem.* **121**: 969–973.
21. Kharel, Y., T. Huang, A. Salamon, T. E. Harris, W. L. Santos, and K. R. Lynch. 2020. Mechanism of sphingosine 1-phosphate clearance from blood. *Biochem. J.* **477**: 925–935.
22. Samocha-Bonet, D., V. D. Dixit, C. R. Kahn, R. L. Leibel, X. Lin, M. Nieuwdorp, K. H. Pietilainen, R. Rabasa-Lhoret, M. Roden, P. E. Scherer, et al. 2014. Metabolically healthy and unhealthy obese—the 2013 Stock Conference report. *Obes. Rev.* **15**: 697–708.
23. Vishvanath, L., and R. K. Gupta. 2019. Contribution of adipogenesis to healthy adipose tissue expansion in obesity. *J. Clin. Invest.* **129**: 4022–4031.
24. Skurk, T., C. Alberti-Huber, C. Herder, and H. Hauner. 2007. Relationship between adipocyte size and adipokine expression and secretion. *J. Clin. Endocrinol. Metab.* **92**: 1023–1033.
25. Holland, W. L., R. A. Miller, Z. V. Wang, K. Sun, B. M. Barth, H. H. Bui, K. E. Davis, B. T. Bikman, N. Halberg, J. M. Rutkowski, et al. 2011. Receptor-mediated activation of ceramidase activity initiates the pleiotropic actions of adiponectin. *Nat. Med.* **17**: 55–63.
26. Hardy, O. T., M. P. Czech, and S. Corvera. 2012. What causes the insulin resistance underlying obesity? *Curr. Opin. Endocrinol. Diabetes Obes.* **19**: 81–87.
27. Gustafson, B., S. Gogg, S. Hedjazifar, L. Jenndahl, A. Hammarstedt, and U. Smith. 2009. Inflammation and impaired adipogenesis in hypertrophic obesity in man. *Am. J. Physiol. Endocrinol. Metab.* **297**: E999–E1003.
28. Andersson, C. X., B. Gustafson, A. Hammarstedt, S. Hedjazifar, and U. Smith. 2008. Inflamed adipose tissue, insulin resistance and vascular injury. *Diabetes Metab. Res. Rev.* **24**: 595–603.
29. Frühbeck, G., L. Mendez-Gimenez, J. A. Fernandez-Formoso, S. Fernandez, and A. Rodriguez. 2014. Regulation of adipocyte lipolysis. *Nutr. Res. Rev.* **27**: 63–93.
30. Haczeyni, F., K. S. Bell-Anderson, and G. C. Farrell. 2018. Causes and mechanisms of adipocyte enlargement and adipose expansion. *Obes. Rev.* **19**: 406–420.
31. Ballestri, S., F. Nascimbeni, E. Baldelli, A. Marrazzo, D. Romagnoli, and A. Lonardo. 2017. NAFLD as a sexual dimorphic disease: role of gender and reproductive status in the development and progression of nonalcoholic fatty liver disease and inherent cardiovascular risk. *Adv. Ther.* **34**: 1291–1326.
32. Qi, Y., J. Chen, A. Lay, A. Don, M. Vadas, and P. Xia. 2013. Loss of sphingosine kinase 1 predisposes to the onset of diabetes via promoting pancreatic beta-cell death in diet-induced obese mice. *FASEB J.* **27**: 4294–4304.
33. Allende, M. L., M. Bektas, B. G. Lee, E. Bonifacino, J. Kang, G. Tuymetova, W. Chen, J. D. Saba, and R. L. Proia. 2011. Sphingosine-1-phosphate lyase deficiency produces a pro-inflammatory response while impairing neutrophil trafficking. *J. Biol. Chem.* **286**: 7348–7358.
34. Zamani, N., and C. W. Brown. 2011. Emerging roles for the transforming growth factor-[beta] superfamily in regulating adiposity and energy expenditure. *Endocr. Rev.* **32**: 387–403.
35. Tan, C. K., N. Leuenberger, M. J. Tan, Y. W. Yan, Y. Chen, R. Kambadur, W. Wahli, and N. S. Tan. 2011. Smad3 deficiency in mice protects against insulin resistance and obesity induced by a high-fat diet. *Diabetes.* **60**: 464–476.
36. Trojanowska, M. 2009. Noncanonical transforming growth factor beta signaling in scleroderma fibrosis. *Curr. Opin. Rheumatol.* **21**: 623–629.
37. Sato, M., M. Markiewicz, M. Yamanaka, A. Bielawska, C. Mao, L. M. Obeid, Y. A. Hannun, and M. Trojanowska. 2003. Modulation of transforming growth factor-beta (TGF-beta) signaling by endogenous sphingolipid mediators. *J. Biol. Chem.* **278**: 9276–9282.
38. Hajer, G. R., T. W. v. Haefen, and F. L. Visseren. 2008. Adipose tissue dysfunction in obesity, diabetes, and vascular disease. *Eur. Heart J.* **29**: 2959–2971.
39. Haemmerle, G., A. Lass, R. Zimmermann, G. Gorkiewicz, C. Meyer, J. Rozman, G. Heldmaier, R. Maier, C. Theussl, and S. Eder. 2006. Defective lipolysis and altered energy metabolism in mice lacking adipose triglyceride lipase. *Science.* **312**: 734–737.
40. Schweiger, M., M. Romauch, R. Schreiber, G. F. Grabner, S. Hütter, P. Kotzbeck, P. Benedikt, T. O. Eichmann, S. Yamada, and O. Knittelfelder. 2017. Pharmacological inhibition of adipose triglyceride lipase corrects high-fat diet-induced insulin resistance and hepatosteatosis in mice. *Nat. Commun.* **8**: 14859.
41. Schreiber, R., H. Xie, and M. Schweiger. 2019. Of mice and men: the physiological role of adipose triglyceride lipase (ATGL). *Biochim. Biophys. Acta Mol. Cell Biol. Lipids.* **1864**: 880–899.
42. Yang, A., and E. P. Mottillo. 2020. Adipocyte lipolysis: from molecular mechanisms of regulation to disease and therapeutics. *Biochem. J.* **477**: 985–1008.
43. Azzu, V., M. Vacca, S. Virtue, M. Allison, and A. Vidal-Puig. 2020. Adipose tissue-liver cross talk in the control of whole-body metabolism: implications in non-alcoholic fatty liver disease. *Gastroenterology.* **158**: 1899–1912.
44. Koeck, E. S., T. Iordanskaia, S. Sevilla, S. C. Ferrante, M. J. Hubal, R. J. Freishtat, and E. P. Nadler. 2014. Adipocyte exosomes induce transforming growth factor beta pathway dysregulation in hepatocytes: a novel paradigm for obesity-related liver disease. *J. Surg. Res.* **192**: 268–275.